Photodiagnosis and Photodynamic Therapy 30 (2020) 101662

Contents lists available at ScienceDirect

Photodiagnosis and Photodynamic Therapy

journal homepage: www.elsevier.com/locate/pdpdt

Photodynamic treatment with cationic Ir(III) complexes induces a synergistic antimicrobial effect with imipenem over carbapenem-resistant *Klebsiella pneumoniae*

Manuel Valenzuela-Valderrama[a], Vanessa Bustamante[a], Nicolás Carrasco[a], Iván A. González[b], Paulina Dreyse[c], Christian Erick Palavecino[a,*]

[a] Laboratorio de Microbiología Celular, Instituto de Investigación e Innovación en Salud, Facultad de Ciencias de la Salud, Universidad Central de Chile, Chile
[b] Instituto de Investigación e Innovación en Salud, Facultad de Ciencias de la Salud, Universidad Central de Chile, Chile
[c] Departamento de Química, Universidad Técnica Federico Santa María, Av. España 1680, Casilla 2390123, Valparaíso, Chile

ARTICLE INFO

Keywords:
Klebsiella pneumoniae
KPC
MDR
Photodynamic therapy
Antimicrobial photodynamic therapy

ABSTRACT

Background: Bacteria prevalent in the hospital environment have developed multi-drug resistance (MDR), such as the carbapenemase-producing *Klebsiella pneumoniae* (KPC^+). Photodynamic therapy (PDT), which uses light-activated photosensitizer compounds (PSs), has emerged as an alternative to antibiotics. Cationic-PSs have a better bactericidal effect by interacting more closely with the bacterial envelope.

Methods: Two PSs based on cationic Ir (III) compounds (PSIR-1 and PSIR-2) were studied in photodynamic therapy against KPC^+ and KPC^- bacteria, and their PDT activities were compared with a cationic Ru(II) control compound (PS –Ru).

Results: Similar to the behavior of PS-Ru control, the cytotoxicity of PSIR-1 and 2, showing a bacterial inhibition growth of more than $3\log_{10}$ (> 99.9 % inactivation), at light fluency of 17 μW/cm^2. The minimal dose to accomplish the inhibition in $3\log_{10}$ was determined for PSIR-1 and PSIR-2 at 4 and 2 μg/mL, respectively and the lethality was 30 min of light exposure for both compounds. Notably, the PSIR-1 and 2 compounds showed a synergistic effect with imipenem by significantly increasing (up to 6 $\log_{10}$) the photodynamic bactericidal effect for KPC^+ strains. This synergy is specific for PSIR-1 and 2 compounds, since it was not observed with the PS-Ru control. On normal gastric cells GES-1, both PSIR-1 and 2 showed significant cytotoxicity; however, the highest cytotoxicity was found in gastric tumor cells (AGS).

Conclusion: The compounds PSIR-1 and 2 are bactericidal photosensitizers and represent a promising alternative for complementing the treatment of infections by MDR bacteria since they should not be toxic in the dark.

1. Introduction

The most prevalent pathogenic bacteria in hospital environments, such as producers of healthcare-associated infections (HAIs), have developed a high resistance to antibiotics (MDR) [1]. The world health organization (WHO) considers the MDR bacteria as one of the pressing global threats to human health in the 21st century and described the situation as a global crisis and an impending catastrophe of a return to the pre-antibiotic era [2]. In this regard, the WHO published a list of the microorganisms that should be investigated with priority to generate new antimicrobial drugs [3]. This enlistment considers as a critic, in first priority, the MDR Enterobacteriaceae producing extended-spectrum β-lactamase (ESBL) plus carbapenemase [3,4]. Among them, stand out *Klebsiella pneumoniae,* which is associated with urinary tract infections (UTI), and pneumonia [5,6]. The MDR *K. pneumoniae* strains are also one of the major (30 %) producers of health-associated infections (HAIs) [7,8]. Strains of *K. pneumoniae* producing carbapenemases (KPC^+) cause serious infections that result in high mortality that can reach 30–70 % [9–11]. The only therapeutic option to treat severe KPC^+ infections is reduced to polymyxin, such as colistin, and tigecycline antibiotics [12]. However, in 2016, was reported the polymyxin resistance gene, *mcr*-1, which is plasmid-encoded, significantly

* Corresponding author at: Laboratorio de Microbiología Celular, Facultad de Ciencias de la Salud, Universidad Central de Chile, Lord Cochrane 418, 3° piso Santiago, 8330546, Chile.
E-mail addresses: manuel.valenzuela@ucentral.cl (M. Valenzuela-Valderrama), vanessa.bustamante@alumnos.ucentral.cl (V. Bustamante), carrascov@alumnos.ucentral.cl (N. Carrasco), ivan.gonzalez@ucentral.cl (I.A. González), paulina.dreyse@usm.cl (P. Dreyse), christian.palavecino@ucentral.cl (C.E. Palavecino).

https://doi.org/10.1016/j.pdpdt.2020.101662
Received 15 October 2019; Received in revised form 6 January 2020; Accepted 10 January 2020
Available online 13 January 2020
1572-1000/

facilitating its dissemination capacity [2]. At present, the *mcr*-1 gene has been reported in several strains of HAI-producing Enterobacteriaceae in numerous countries on five continents [9,11,13].

Considering the high risk of public health due to the deficiency of new antibiotics, new antimicrobial drugs other than antibiotics must be developed. In this sense, photodynamic therapy (PDT) has demonstrated a successful antitumor and antimicrobial activity [14]. However, very few initiatives have explored the antimicrobial activity of PDT against *K. pneumoniae* infections [6,15–17]. The PDT is based on the use of photosensitizer compounds (PS) that produce local cytotoxicity following light activation (photooxidative stress) [18]. The PS compounds absorb the visible light energy of specific wavelength and transfer it to molecular oxygen by electron transferring to produce superoxide ($O_2^{\cdot -}$) or by energy transfer that produces highly reactive singlet oxygen ($^1O_2$). The electron transfer process that produces $O_2^{\cdot -}$ is called the Type I effect, and the energy transfer process that produces $^1O_2$ is called the Type II effect, being this last that provide most of the photooxidative stress [19,20]. The $^1O_2$ is a reactive oxygen species (ROS) that produce concerted addition reactions to alkene groups present in proteins or lipids, resulting in non-specific bacterial death [14,19]. The generation of $^1O_2$ will be effective, considering many properties of the PSs, where a longer lifetime of their excited states is essential in order to enhance the probability to interact with the triplet oxygen and produce the $^1O_2$ [21–24]. On the other hand, a more intimate relationship between PSs molecules and the negative bacterial envelope, improve the effect produced by photooxidative stress [25]. In this regard, cationic PSs have demonstrated a better photodynamic effect than anionic PSs, on *K. pneumoniae* [16]. Keeping this in mind, the cationic Ir(III) compounds of the type $[Ir(C^N)_2(N^N)](PF_6)$, with N^N = 1-methyl-1H-pyrazole [3′,4′:5,6]pyrazino [2,3-f][1,10]phenanthroline, were used as photosensitizers for PDT. The compound with 2-phenylpyridine as C^N ligand was denominated PSIR-1, and with 2-(2,4-difluorophenyl)pyridine was designated PSIR-2 (see Fig. 1) [26,27]. We compared our results with the activity of a control compound, $[Ru(bpy)_3](PF_6)_2$, which we call PS-Ru since it has lifetimes in an excited state comparable to our compounds, that show metal to ligand charge transfer (MLCT) at 450 nm [28]. We determined the pharmacological qualities of our PSs, such as the minimum effective concentration and the minimum time of exposure to light necessaries to achieve a therapeutic effect [29]. We also evaluated their usefulness as a complementary therapy, and we verified whether it produces synergism with the antibiotic of choice for the antimicrobial treatment against MDR *Klebsiella pneumoniae*. Finally, since these compounds should be used in the treatment of infections *in vivo*, their dark cytotoxicity was evaluated on eukaryotic cells, such as normal gastric cells (GES-1) and tumor gastric cells (AGS).

2. Materials and methods

2.1. Photosensitizers characterization

We used two coordination compounds that were previously synthesized, whose photodynamic effect has not been characterized. Details about the synthesis and photophysical characterization are reported in the literature [26]. These compounds are based on Ir(III) with $[Ir(C^N)_2(N^N)](PF_6)$ as general formula, where N^N is the ancillary ligand, and in this case, 1-methyl-1H-pyrazole [3′,4′:5,6]pyrazino [2,3-f][1,10]phenanthroline is used. The C^N corresponds to a cyclometalating ligand, then, using 2-phenylpyridine as C^N, the compound was denominated PSIR-1, and with 2-(2,4-difluorophenyl)pyridine the compound was called PSIR-2 [26]. The structure and purity of the compounds were confirmed by nuclear magnetic resonance (NMR), Fourier-*transform infrared spectroscopy* (FT-IR), and high-resolution mass spectroscopy (HRMS). The absorption spectra were measured in suitable solutions using a Shimadzu UV–vis Spectrophotometer UV-1900. The molar extinction coefficients of the characteristic bands were determined from the absorption spectra. Photoluminescence spectra were taken on an Edinburgh Instrument spectrofluorometer. Solutions of the compounds were previously degassed with N_2 for approximately 20 min. The emission quantum yields (Φ_{em}) were calculated according to the description of the literature [30].

2.2. Antimicrobial activity of photosensitizers compounds

Purified powder preparation of PSIR-1 and 2 compounds were solubilized as a stock solution in acetonitrile at 2 mg/mL. From these, aqueous solutions were prepared at indicated concentrations in cation adjusted Muller Hinton (ca-MH) broth. *K. pneumoniae* strains KPPR1 (KPC^-) and ST258 (KPC^+) were kindly gifted by Dr. Susan Bueno (Pontificia Universidad Católica de Chile). All bacteria were growth as axenic culture in Luria Bertani broth or agar medium as convenient. Photodynamic experiments were performed in a final volume of 500 μL of ca-MH broth per well into 24 well plates mixing 1×10^7 colony forming units (CFU) of each bacterial strains whit each photosensitizer. Control wells with bacteria culture but with no photosensitizer were included. In every experiment, each group was performed in triplicate into the 24 well plates, and a minimum of three replicas of each experiment was performed, giving an $n = 9$. For light exposure, a chamber with a white LED lamp was used at a photon flux of 17 μW/cm^2. The temperature inside the chamber was controlled using a mercury thermometer, and no rise in temperature was registered. After the light exposure, bacteria were recovered, and CFU of viable bacteria was determined by broth-micro dilution and sub-cultured on ca-MH agar plates. Agar plates were incubated at 37 °C and colony counting was registered using a stereoscopic microscope after 16 − 20 h incubation as recommended by the Clinical and Laboratory Standards (CLSI) for antimicrobial susceptibility testing [31]. The minimal effective concentration of each photosensitizer was determined by exposing a constant bacterial suspension (1×10^7 CFU/mL) to different concentrations of each PS. To determine the lethality, 16 μg/mL of each photosensitizer was incubated with 1×10^7 CFU/mL of bacteria and exposed to different times of light. Control groups were not mixed with any PS, exposed to light, and recovered at the same time points than mixed bacteria. Subsequently, viable bacteria were enumerated by serial micro-dilution as above.

2.3. Cell culture

The human gastric cancer cell line AGS (ATCC CRL-1793) and the human immortalized gastric cell line GES-1 (kindly provided by Dr. Dawit Kiane, University of Texas, USA), were cultured in RPMI 1640 without antibiotics, supplemented with 10 % FBS and 5 % CO_2 atmosphere. Starting cultures of 2×10^7 cells incubated in triplicate in a 24 well plate for 24–48 h until 70–90 % confluence.

2.4. Cytotoxicity assays

The dark cytotoxicity effect for AGS and GES-1 cells was determined in 24 well plates exposed to indicated concentrations of each PSIR-1 or 2 compounds for 1 h at 37 °C in darkness. After incubation, the PS compound was removed by washing the cells with 1 mL of D-PBS twice and incubated without PSs for 24 h under the same conditions in complete medium. A control group of untreated cells was included. After incubation, treated and untreated control cells were trypsinized and performed counting of death cell by trypan blue exclusion in a hemocytometer chamber or viability by MTS assay (Promega) following the manufacturer's instructions.

2.5. Statistical analysis

GraphPad Prism version 6.0 software was used to perform statistical analyses and graphs. Statistical significance was assessed using *one-way*

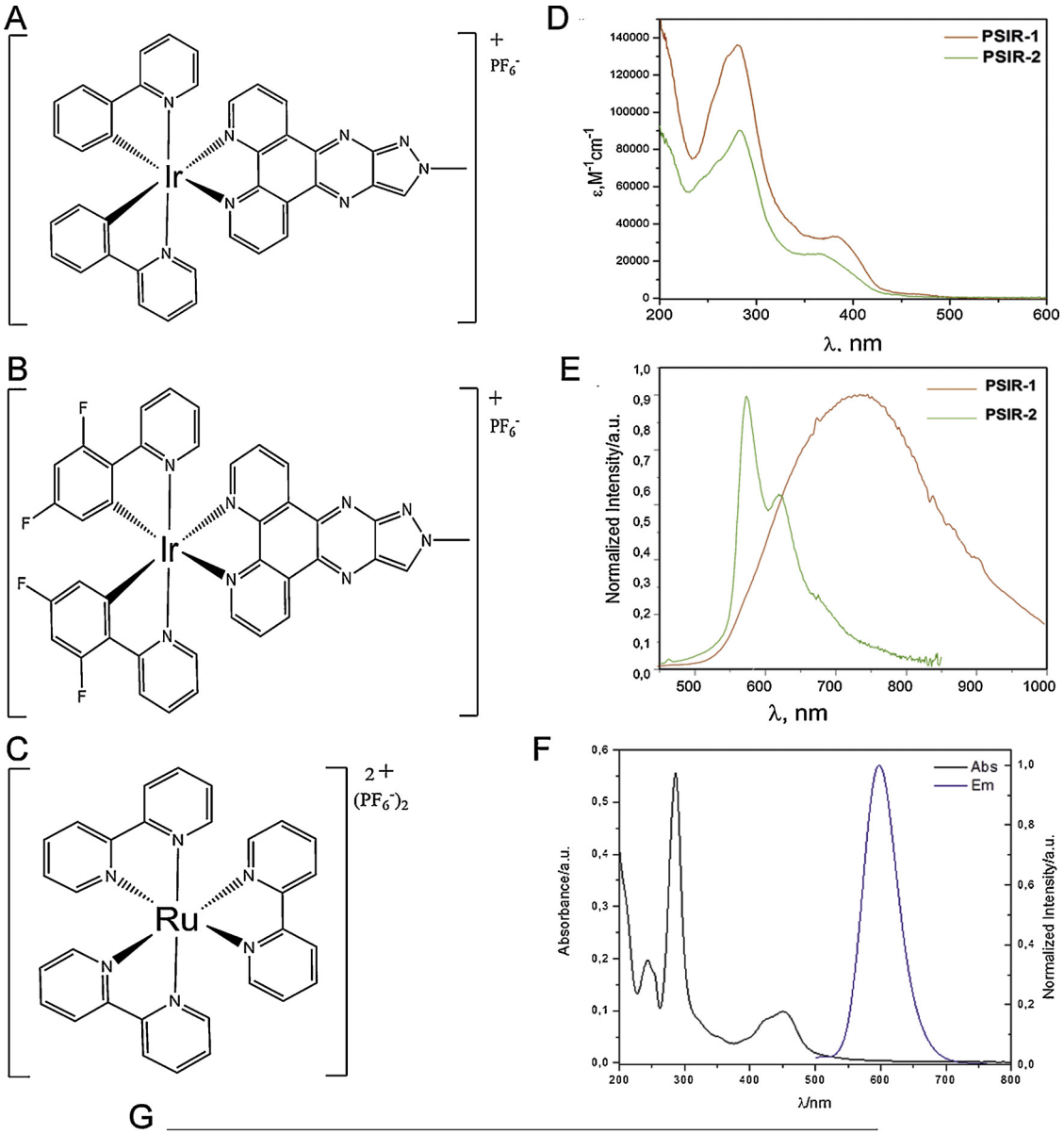

G

Compounds	λ_{abs} /nm	λ_{em}/nm	Φ_{em}	τ/μs
PSIR-1	383	738	0.004	0.18
PSIR-2	365	573, 620	0.010	0.97
PS-Ru	300, 450	600	0.095	0.86

Fig. 1. Photosensitizer Compounds and their Photophysical Characterization. Chemical structures of Ir(III) complexes PSIR-1 **A** and PSIR-2 **B,** and the Ru(II) control compound **C.** The photophysical characterization for both Ir(III) PS compounds by absorption **D**, and emission **E,** in acetonitrile solutions. The photophysical characterization for Ru(II), absorption (black line) and emission (blue line) **F**. The quantum yields and lifetimes in degassed acetonitrile solutions of each PSs **G**.

ANOVA and the Tukey post-test for the lethality curve or the *T*-test for pairing groups.

3. Results

3.1. Photophysical and electrochemical properties of the cationic Ir(III) compounds

In this work, two coordination compounds were tested for its utility in photodynamic therapy against *K. pneumoniae*. Because the literature demonstrates that cationic compounds are more effective against bacteria [16], the selected Ir(III) compounds are characterized by a positive charge into the first coordination sphere (Fig. 1) [26]. These PSs are cyclometalated compounds based on Ir(III) and polypyridine ligands; the specific molecules are $[Ir(ppy)_2(N^{\wedge}N)](PF_6)$ for PSIR-1, and $[Ir(F_2ppy)_2(N^{\wedge}N)](PF_6)$ for PSIR-2, where N^N = 1-methyl-1H-pyrazole [3′,4′:5,6]pyrazino [2,3-f][1,10]phenanthroline (Fig. 1A and B) [26]. The photophysical evaluation for PSIR-1 and 2 in acetonitrile solutions showed that both have similar absorption processes around 285 nm and at 383 nm (PSIR-1) and 365 nm (PSIR-2) (Fig. 1D) [26]. When the compounds were excited with a wavelength corresponding to the lowest absorption energy, the PSs showed emission with a maximum at 738 nm for PSIR-1 and at 573 and 620 nm for PSIR-2 (Fig. 1E), and the lifetimes registered of these excited states were 0.18 and 0.97 μs,

respectively (Fig. 1G). The calculated quantum yield (Φ_{em}) was 0.004 for PSIR-1 and 0.010 for PSIR-2 [26] (Fig. 1G). Related to the PSs commonly used to generation of singlet oxygen, the organic molecules are highlighted, as phenalenone and Rose Bengal, and also some Ru(II) compounds and macrocycles (porphyrins and phthalocyanines) [32–34]. For this purpose, the use of Ir(III) cyclometalated compounds have been little explored [35], therefore, considering the attractive photophysical and structural characteristics of PSIR-1 and PSIR-2, these were selected as promising PSs to be evaluated in the photodynamic antimicrobial activity; and their activities were compared to the PS compound $[Ru(bpy)_3](PF_6)_2$ which we call PS-Ru. Therefore, Fig. 1 depicted the chemical structure of PS-Ru (Fig. 1C), and their photophysical analysis of absorption and emission spectra (Fig. 1F). According to the literature, the PS-Ru showed absorption processes at 300 nm and 450 nm (black line), and maximum emission at 600 nm when excited at the MLCT band of 450 nm (blue line) [30]. The Φ_{em} is 0.095 [30] and the lifetimes registered of its excited states is 0.855 μs [28] (Fig. 1G).

3.2. Photodynamic antimicrobial activity of the PSIR-1 and PSIR-2 compounds

To determine whether the PSIR-1 and 2 compounds have photodynamic antimicrobial activity, their ability to inhibit the bacterial growth were tested *in vitro*. Two strains of *K. pneumoniae* were used; the imipenem sensitive (KPC^-) sequenced strain, KPPR1, and the imipenem resistant (KPC^+) typo strain, ST258. The antimicrobial activity of the PSIR-1 and PSIR-2 compounds was compared with the antimicrobial activity of the reference PS-Ru compound, as a positive control [17,36–38]. In the initial screen, each compound was tested at a concentration of 16 μg /mL to determine if any growth-inhibitory effects were evident in comparison to the vehicle (acetone 0.1 %) control. As seen in Fig. 2, in comparison with the control of untreated bacteria (red bars), the photodynamic treatment with 16 μg/mL of PSIR-1 or PSIR-2 (yellow bars) inhibited in 3 $\log_{10}$ (> 99.9 % inactivation) the bacterial growth of both strains of *K. pneumoniae*, KPPR1 and ST258 (** $p < 0.01$). The results showed that the inhibition of bacterial growth produced by PSIR-1 and 2 is a photodynamic effect since the compounds are not toxic in the absence of light (orange bars) ($ns = p > 0.05$; compared to untreated control). Therefore, both PSIR-1 and PSIR-2 need to be activated by light to exhibit their bacterial growth inhibitory effect. Similar results were obtained when bacteria were treated using the PS-Ru control, as the bacterial growth inhibition was observed only after light activation ($p < 0.05$). However, it should be noted that the PSIR-1 and 2 compounds achieved an improved inhibitory effect on the bacterial load of at least 1$\log_{10}$, compared to that obtained by the PS-Ru control.

3.3. Determination of the minimum effective concentration of PSIR-1 and PSIR-2

To be used as an *in vivo* treatment, photodynamic compounds should ideally be used in low concentrations and should be excited with short light periods [18]. Two pharmacologic aspects of the photodynamic activity were evaluated for the PSIR-1 and PSIR-2 compounds; their minimum effective concentration, and the minimum light exposition time, lethality. The study was performed in the two strains of *K. pneumoniae*, KPPR1 and St258. To determine the minimum effective concentration, 1 × 10^7 bacteria from each strain solubilized in 1x PBS and were mixed with concentrations ranging from 0.25–32 μg/mL of each PS. The mix was exposed to 17 μW/cm^2 of white led light for 1 h at room temperature. The control groups were not mixed with any PS (0 μg/mL) but exposed to light under the same conditions. Viable bacteria were subsequently enumerated by serial micro-dilution and colony count in ca-MH agar. The minimum effective concentration was established as the concentration at which the bacterial load decreased by

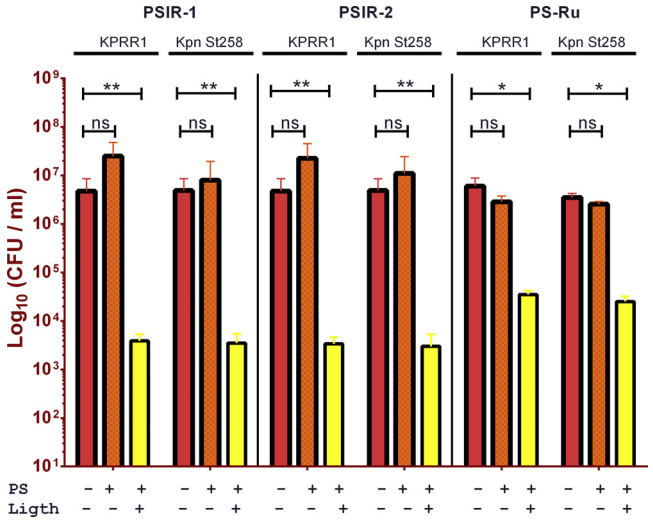

Fig. 2. Photodynamic antimicrobial capability of PSIR-1 and 2. Two strains of *K. pneumoniae* were used; the imipenem sensitive sequenced strain (KPC^-) (KPRR1) and the imipenem resistant typo strain (KPC^+) ST258. The bacteria were used at a concentration of 1 × 10^7 CFU/mL and mixed in triplicate with 16 μg/mL of PSIR-1 or PSIR-2 compounds. For the PDT, the mixture of bacteria and PS were exposed for 1 h at 17 μW/cm^2 with light (yellow bars). As a control, bacteria combined with the PSs but not exposed to light (orange bars) and bacteria not combined with the PSs (red bars) were included. Viable bacteria were enumerated by colony count on ca-MH agar after serial micro-dilution. The CFU/mL values are presented as means ± SD, on a $\log_{10}$ scale. Not significant [ns] $p > 0.05$ by Student's *t*-test among bacteria treated with PS without light compared to untreated control bacteria; * $p < 0.05$, ** $p < 0.01$ by Student's *t*-test among bacteria treated with PS exposed to light compared to untreated control bacteria.

99.9 % (3 $\log_{10}$). As shown in Fig. 3A and B, the minimum effective concentration determined for PSIR-1 was 4 μg/mL, and for PSIR-2 was 2 μg/mL, respectively. Lethality was determined for 1 × 10^7 UFC/mL of each strain solubilized in 1x PBS mixed with 16 μg/mL of each PS and exposed for 5, 15, 30, 60, and 120 min at 17 μW/cm^2 of white led light. Control wells with bacteria without PSs were also included. Subsequently, viable bacteria were enumerated by serial micro-dilution and colony count in ca-MH agar. The lethality time was established as the time in minutes at which the bacterial load decreased by 99.9 % (3 $\log_{10}$). As shown in Fig. 3C, for PSIR-1, although there was a significant reduction ($p < 0.05$) in bacterial load after 30 min of light exposure, it was at 60 min when the threshold of 3 $\log_{10}$ was reached. In comparison, as shown in Fig. 3D, for PSIR-2, the threshold of 3 $\log_{10}$ was reached at 30 min of exposure time ($p < 0.05$).

3.4. Photodynamic synergistic effect with imipenem of PSIR-1 and PSIR-2 compounds

Since carbapenems are the chosen therapy for many multi-drugs resistant enterobacteria, we decided to verify *in vitro* if photodynamic treatment could improve the effectiveness of this antibiotic. For this, the strains of *K. pneumoniae* sensitive to carbapenem KPC^- (KPPR1) and the resistant strain KPC^+ (ST258) were exposed to a mixture of 4 μg/mL of imipenem with 4 or 2 μg/mL of each PSIR-1 or 2 respectively. Control bacteria without imipenem and exposure to light were included. Remarkably, both PSIR-1 and 2 compounds shown a synergistic effect with imipenem, as the combined treatment significantly (*** $p < 0.001$) increased from 3 to 6 $\log_{10}$ the bactericidal effect for the KPC^+ strain (Fig. 4). This synergistic behavior was not observed when combining the imipenem with the PS-Ru control compound.

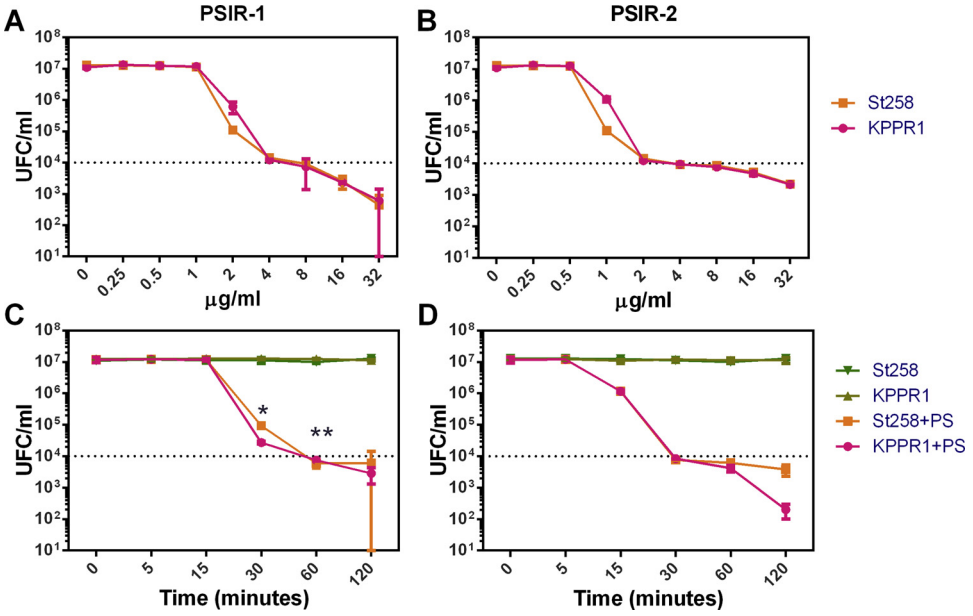

Fig. 3. Determination of minimum effective concentration and time lethality. Two strains of *K. pneumoniae* were used; KPRR1 and ST258 at 1 × 10^7 CFU/mL. To determine the minimum effective concentration, the bacteria were mixed with increasing concentrations (0.25–32 µg/mL) of the compounds PSIR-1 **A,** or PSIR-2 **B,** and exposed for 1 h to 17 µW/cm^2 of white led light. The time lethality was determined, mixing the bacteria with 16 µg/mL of PSIR-1 **C,** or PSIR-2 **D,** and exposure for increasing times (5, 15, 30, 60 and 120 min) to 17 µW/cm^2 of white led light. Viable bacteria were enumerated by colony count on ca-MH agar after serial-microdilution. The CFU/mL values are presented as means ± SD, on a $\log_{10}$ scale (* $p < 0.05$, ** $p < 0.01$ by Student's *t*-test among bacteria treated with PS exposed to light compared to untreated control bacteria).

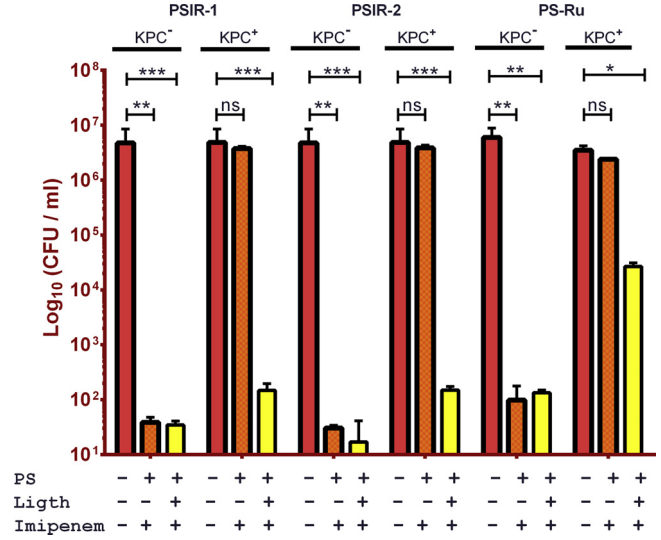

Fig. 4. Photodynamic synergistic effect with imipenem. 1 × 10^7 CFU/mL of the sensitive strain, KPC$^-$ (KPPR1), and the resistant strain, KPC$^+$ (ST258), to carbapenem of *K. pneumoniae*, were exposed to a mixture of 4 µg/mL of imipenem and with 4 µg/mL of each PS. For the PDT, the bacteria in the presence of the mixture PS + imipenem were exposed for 1 h at 17 µW/cm^2 of light (yellow bars). Controls include bacteria that, in the presence of imipenem whose PS was not activated by light (orange bars) and bacteria not combined with imipenem nor PSs (red bars). Viable bacteria were enumerated by colony count on ca-MH agar after serial microdilution. The CFU/mL values are presented as means ± SD, on a $\log_{10}$ scale. Not significant [ns] $p > 0.05$ by Student's *t*-test among bacteria treated with PS + imipenem without light compared to untreated control bacteria; * $p < 0.05$, ** $p < 0.01$, *** $p < 0.001$ by Student's *t*-test among bacteria treated with PS + imipenem exposed to light compared to untreated control bacteria.

3.5. Dark cytotoxic effect of PSIR-1 and PSIR-2 over eukaryotic cells

Since photodynamic therapy is intended to treat infections *in vivo*, photosensitizer compounds must be safe when they come into contact with the patient's eukaryotic cells [18]. In this work, the dark cytotoxicity of the compounds PSIR-1 and PSIR-2 was tested in two cell lines; gastric cells derived from a metaplastic gastric cancer, AGS, and transformed gastric cells, GES-1. Two parameters of cytotoxicity were determined; the reduction of cell proliferation and cell death. For the determination of cell proliferation, semi-confluent cultures of each cell line were incubated in the dark for 1 h with; 1, 2, 4, 8, and 16 µg/mL of each PS. The cells were subsequently washed with 1x PBS, and complete medium was added to incubate the cells for 24 h at 37 °C in a 5 % CO_2 atmosphere. Cell proliferation was determined by MTS assays using 5000 treated cells per well in 96-well plates. As seen in Fig. 5A, during the MTS test, AGS cells treated with PSIR-1 (black bars) shown a dose-dependent reduction on viability from 50 % with 1 µg/mL of PS compound ($p < 0.001$) to less than 10 % with 16 µg/mL of PS compound ($p < 0.0001$). In contrast, for GES-1 cells (grey bars), a non-significant reduction to 83 % with 1 µg/mL ($p > 0.05$) was observed, although, higher concentrations produced significant reductions to less than 50 % at 16 µg/mL ($p < 0.0001$). Similar results were observed when PSIR-2 compounds were used (Fig. 5B) over AGS cells (black bars). A dose-dependent significant reduction in proliferative activity was observed from 1 µg/ml. Although the PSIR-2 compound induced a significant death of the GES-1 exposed cells, it did not exceed 35 % when exposed to amounts between 1–4 µg/mL ($p < 0.01$). Quantities of 8 or 16 µg/mL reduced the proliferation of exposed cells by 50 and 90 %, respectively ($p < 0.0001$).

For the determination of cell death, 40,000 cells were exposed to 2 or 4 µg/mL of PSIR-1 or PSIR-2 in darkness for 1 h at 37 °C. After incubation, the cells were washed with D-PBS, complete medium was added and incubated in the dark at 37 °C. After 24 h incubation, the cells were trypsinized and determined death cells by the exclusion of trypan blue in a hemocytometer chamber. As seen in Fig. 6, when AGS cells (black bars) were exposed to 2 µg/mL of PSIR-1, live cells were significantly reduced to 86 % ($p < 0.01$). When the dose increased to 4 µg/mL, the live cells were reduced to 62 % ($p < 0.01$). In comparison, there was no dose-dependence on the effect of PSIR-2 on cell death, where both concentrations significantly reduced living cells to around 70 % ($p < 0.01$). Similarly, when GES-1 cells (grey bars) were exposed to 2 or 4 µg/mL of PSIR-1, a significant reduction in live cells were observed to approximately 68 % ($p < 0.01$). In comparison, exposure of GES-1 to PSIR-2 induced a significant dose-dependent decrease in cell life at 60 and 55 % for 2 and 4 µg/mL, respectively ($p < 0.01$).

4. Discussion

Since the proliferation of MDR bacteria constitutes a severe risk to human health [2], consequently, the therapeutic alternatives to treat

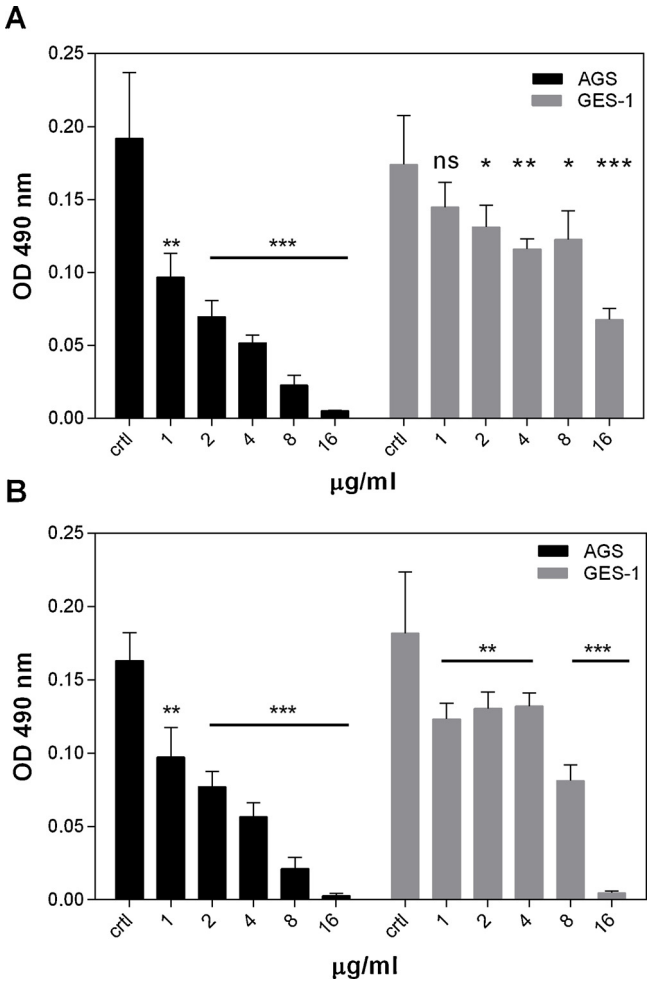

Fig. 5. Dark cytotoxicity of PS compounds in the proliferation of eukaryotic cells. AGS and GES-1 gastric cells were exposed to increasing concentrations of each compound PSIR-1 **A,** or PSIR-2 **B**. The proliferative capacity of the cells was determined by MTS assays. The results are the mean ± SD of the optical density measured at 490 nm (Not significant [ns]$p > 0.05$, *$p < 0.05$, **$p < 0.01$, ***$p < 0.001$, by Student's *t*-test between cells treated with PSs compared to untreated control cells (0 µg/ml)).

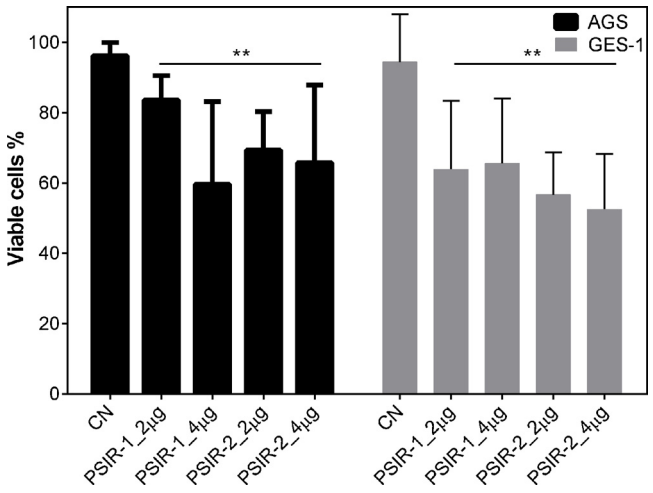

Fig. 6. Measurement of eukaryotic cell death by dark cytotoxicity of PS compounds. AGS and GES-1 gastric cells were exposed to 2 or 4 µg/mL of each PSIR-1 or PSIR-2 compound, and cell viability was determined by exclusion with trypan blue in a hemocytometer chamber. The results are the mean ± SD of the percentage of living cells (** $p < 0.001$, by Student's *t*-test among cells exposed to PSs compared to control untreated cells).

infections are depleted [3]. Then, the use of complementary therapies becomes viable, not just to save the lives of those patients where no antibiotics are available, but also to reverse bacteria resistance, reducing the increase of MDR strains. In this work, we were able to prove the usefulness of two photosensitizer compounds based on Ir(III) in photodynamic therapy against pathogenic bacteria. The *K. pneumoniae* model was chosen because it is one of the MDR bacteria with the highest presence as a producer of HAIs [3,6]. Because the photodynamic therapy is nonspecific, the Ir(III) compounds could also be useful in the treatment of other clinically relevant bacteria [6].

On the other hand, since the bacteria envelopes are negatively charged, these selected compounds have a positive charge that theoretically should improve photodynamic activity, allowing better molecular proximity [25]. As the cationic compounds should interact (electrostatically) more strongly with the anionic bacterial envelope, it is expected a weak interaction with the mammalian cell membrane that is almost neutral [25]. Our cationic compounds are shown to be active over *K. pneumoniae*, for photodynamic treatment [16], in a similar manner than bactericidal peptides such as defensins [39]. Evidence that cationic compounds such as PSIR-1 and PSIR-2 can show greater efficiency is the increased efficiency demonstrated by cationic Zn(II) phthalocyanines inactivating *E. coli* and *K. pneumoniae* (KPC^+) bacteria, rather than neutral Zn(II) phthalocyanines [16]. Therefore, the chemical nature of photosensitizer will determine how efficient it is the interaction between the PS and the bacterial envelope [15,40]. Another attractive photophysical properties of the selected Ir(III) compounds PSIR-1 and PSIR-2 is the long lifetimes of their excited states, which could be favorable to promote a better interaction with triplet oxygen to produce singlet oxygen. Consequently, the increased bactericidal activity of PSIR-2 ($\tau = 0.97$ µs) is in agreement with the lifetime values, compared to the behavior of PSIR-1 ($\tau = 0.18$ µs).

The compounds PSIR-1 and PSIR-2 have an excellent bactericidal activity when used in PDT, with > 99.9 % inactivation, comparable to other photodynamic PSs compounds against Gram-negative bacteria [29,41–43]. But more remarkable, those compounds showed a synergistic effect when used in PDT in combination with imipenem, unlike the ruthenium control that did not. The increased bactericidal activity of PSIR-1 and PSIR-2, when combined with antibiotic to > $6\log_{10}$, is comparable to the synergistic effect between conventional antibiotics and alternative compounds that have been reported previously with anti-biofilm peptides in a murine model against ESKAPE pathogens [44]. Because the ruthenium control does not show synergy with antibiotics, this effect should be specific to the chemical formulation underly the PSIR-1 and PSIR-2 compounds. This performance can be understandin-g due to the chemical structure of the N^N ligand in the Ir (III) compounds used (PSIR-1 and PSIR-2), which has an incremented aromaticity and also heteroatoms (N) which could be to favor the interaction of PSIR-1 and PDIR-2 with the bacterial enveloped, compared to the simpler chemical structure of the reference compound of PS-Ru [30]. This synergistic effect is noteworthy since bacteria resistant to a particular antibiotic, imipenem, in this case, can be treated with this antibiotic eliminating the need for rescue therapy.

The two compounds PSIR-1, and PSIR-2 tested in this work are photosensitizers, since inhibition of the growth of both strains of *K. pneumoniae* occurred only after exposure to light. Being its photodynamic antimicrobial activity dependent on light activation, it should not be toxic or show reduced toxicity in the dark. However, the compounds showed a low but significant cytotoxicity in experiments *in vitro*. This cytotoxicity on cells in culture is low compared to that produced by antitumor drugs [45]; then, the compounds could be used *in vivo*. Regardless of the above, the compounds must be tested *in vivo*, for example, in a murine model to establish whether, in the context of the tissues, they may buffer the cytotoxic effect [46]. Also, most of the

cytotoxic effect was observed over replicative neoplastic cells, behavior that has already been reported, in the generation of photodynamic therapies against cancer [18].

5. Conclusions

In summary, although a more exhaustive pharmacological characterization of the PSIR-1 and PSIR-2 compounds is required, these compounds should meet the characteristics necessary to help treat bacterial infections *in vivo*. The compounds PSIR-1 and PSIR-2 demonstrated a bactericidal activity dependent on light activation, which can be used in concentrations in the biological range, similar to antibiotics [31]. The synergistic effect is noteworthy since bacteria resistant to particular antibiotics can be treated with these compounds, eliminating the need for rescue therapy.

Declaration of Competing Interest

The authors declare no conflict of interest.

Acknowledgments

We would like to thanks Dr. Susan Bueno from Pontificia Universidad Católica de Chile, to provide the control strains of *K. pneumoniae*, KPPR1, and the typo strain ST258. Authors are supported by grants: UCENCIP2017015 (awarded to C.E.P.), Fondecyt1171615, UCENCIP2016020 (awarded to M.V.V.), UCENCIP2018002, Fondecyt11180185 (awarded to I.A.G.) and USM Project PI_L_18_17 (awarded to P.D.).

References

[1] R. Laxminarayan, A. Duse, C. Wattal, A.K. Zaidi, H.F. Wertheim, N. Sumpradit, et al., Antibiotic resistance-the need for global solutions, Lancet Infect. Dis. 13 (12) (2013) 1057–1098, https://doi.org/10.1016/S1473-3099(13)70318-9.

[2] Y.Y. Liu, Y. Wang, T.R. Walsh, L.X. Yi, R. Zhang, J. Spencer, et al., Emergence of plasmid-mediated colistin resistance mechanism MCR-1 in animals and human beings in China: a microbiological and molecular biological study, Lancet Infect. Dis. 16 (2) (2016) 161–168, https://doi.org/10.1016/S1473-3099(15)00424-7.

[3] C. Willyard, The drug-resistant bacteria that pose the greatest health threats, Nature 543 (7643) (2017) 15, https://doi.org/10.1038/nature.2017.21550.

[4] WHO, WHO Publishes List of Bacteria for Which New Antibiotics Are Urgently Needed, (2017).

[5] R. Podschun, U. Ullmann, *Klebsiella* spp. as nosocomial pathogens: epidemiology, taxonomy, typing methods, and pathogenicity factors, Clin. Microbiol. Rev. 11 (4) (1998) 589–603.

[6] M. Valenzuela-Valderrama, I.A. Gonzalez, C.E. Palavecino, Photodynamic treatment for multidrug-resistant Gram-negative bacteria: perspectives for the treatment of *Klebsiella pneumoniae* infections, Photodiagn. Photodyn. Ther. 28 (2019) 256–264, https://doi.org/10.1016/j.pdpdt.2019.08.012.

[7] M.K. Paczosa, J. Mecsas, *Klebsiella pneumoniae*: going on the offense with a strong defense, Microbiol. Mol. Biol. Rev. 80 (3) (2016) 629–661, https://doi.org/10.1128/MMBR.00078-15.

[8] W.C. Ko, D.L. Paterson, A.J. Sagnimeni, D.S. Hansen, A. Von Gottberg, S. Mohapatra, et al., Community-acquired *Klebsiella pneumoniae* bacteremia: global differences in clinical patterns, Emerg. Infect. Dis. 8 (2) (2002) 160–166, https://doi.org/10.3201/eid0802.010025.

[9] G.L. Daikos, A. Markogiannakis, M. Souli, L.S. Tzouvelekis, Bloodstream infections caused by carbapenemase-producing *Klebsiella pneumoniae*: a clinical perspective, Expert Rev. Anti. Ther. 10 (12) (2012) 1393–1404, https://doi.org/10.1586/eri.12.138.

[10] P. Tofas, A. Skiada, M. Angelopoulou, N. Sipsas, I. Pavlopoulou, S. Tsaousi, et al., Carbapenemase-producing *Klebsiella pneumoniae* bloodstream infections in neutropenic patients with haematological malignancies or aplastic anaemia: analysis of 50 cases, Int. J. Antimicrob. Agents 47 (4) (2016) 335–339, https://doi.org/10.1016/j.ijantimicag.2016.01.011.

[11] Y. Li, Q.L. Sun, Y. Shen, Y. Zhang, J.W. Yang, L.B. Shu, et al., Rapid increase in prevalence of Carbapenem-Resistant Enterobacteriaceae (CRE) and emergence of colistin resistance Gene mcr-1 in CRE in a Hospital in Henan, China, J. Clin. Microbiol. 56 (4) (2018), https://doi.org/10.1128/JCM.01932-17.

[12] A.K. Pragasam, C. Shankar, B. Veeraraghavan, I. Biswas, L.E. Nabarro, F.Y. Inbanathan, et al., Molecular mechanisms of colistin resistance in *Klebsiella pneumoniae* causing bacteremia from India-a first report, Front. Microbiol. 7 (2016) 2135, https://doi.org/10.3389/fmicb.2016.02135.

[13] R. Wang, L. van Dorp, L.P. Shaw, P. Bradley, Q. Wang, X. Wang, et al., The global distribution and spread of the mobilized colistin resistance gene mcr-1, Nat. Commun. 9 (1) (2018) 1179, https://doi.org/10.1038/s41467-018-03205-z.

[14] A.C. Trindade, J.A. de Figueiredo, S.D. de Oliveira, V.C. Barth Junior, S.W. Gallo, C. Follmann, et al., Histopathological, microbiological, and radiographic analysis of antimicrobial photodynamic therapy for the treatment of teeth with apical periodontitis: a study in rats' molars, Photomed. Laser Surg. (2017), https://doi.org/10.1089/pho.2016.4102.

[15] L. Huang, G. Szewczyk, T. Sarna, M.R. Hamblin, Potassium iodide potentiates broad-spectrum antimicrobial photodynamic inactivation using photofrin, ACS Infect. Dis. 3 (4) (2017) 320–328, https://doi.org/10.1021/acsinfecdis.7b00004.

[16] M. Miretti, R. Clementi, T.C. Tempesti, M.T. Baumgartner, Photodynamic inactivation of multiresistant bacteria (KPC) using zinc(II)phthalocyanines, Bioorg. Med. Chem. Lett. 27 (18) (2017) 4341–4344, https://doi.org/10.1016/j.bmcl.2017.08.028.

[17] L. Edwards, D. Turner, C. Champion, M. Khandelwal, K. Zingler, C. Stone, et al., Photoactivated 2,3-distyrylindoles kill multi-drug resistant bacteria, Bioorg. Med. Chem. Lett. 28 (10) (2018) 1879–1886, https://doi.org/10.1016/j.bmcl.2018.04.001.

[18] P. Agostinis, K. Berg, K.A. Cengel, T.H. Foster, A.W. Girotti, S.O. Gollnick, et al., Photodynamic therapy of cancer: an update, CA Cancer J. Clin. 61 (4) (2011) 250–281, https://doi.org/10.3322/caac.20114.

[19] K. Briviba, L.O. Klotz, H. Sies, Toxic and signaling effects of photochemically or chemically generated singlet oxygen in biological systems, Biol. Chem. 378 (11) (1997) 1259–1265.

[20] E.C. Ziegelhoffer, T.J. Donohue, Bacterial responses to photo-oxidative stress, Nat. Rev. Microbiol. 7 (12) (2009) 856–863, https://doi.org/10.1038/nrmicro2237.

[21] M.C. DeRosa, R.J. Crutchley, Photosensitized singlet oxygen and its applications, Coord. Chem. Rev. 233 (2002) 351–371.

[22] F. Wilkinson, W.P. Helman, A.B. Ross, Quantum yields for the photosensitized formation of the lowest electronically excited singlet state of molecular oxygen in solution, J. Phys. Chem. Ref. Data 22 (1) (1993) 113–262.

[23] P.R. Ogilby, Singlet oxygen: there is indeed something new under the sun, Chem. Soc. Rev. 39 (8) (2010) 3181–3209.

[24] C.S. Foote, Definition of type I and type II photosensitized oxidation, Photochem. Photobiol. 54 (5) (1991) p. 659.

[25] T. Dai, Y.Y. Huang, M.R. Hamblin, Photodynamic therapy for localized infections–state of the art, Photodiagnosis Photodyn. Ther. 6 (3–4) (2009) 170–188, https://doi.org/10.1016/j.pdpdt.2009.10.008.

[26] I. González, M. Natali, A.R. Cabrera, B. Loeb, J. Maze, P. Dreyse, Substituent influence in phenanthroline-derived ancillary ligands on the excited state nature of novel cationic Ir (III) complexes, New J. Chem. 42 (9) (2018) 6644–6654.

[27] R.D. Costa, E. Orti, H.J. Bolink, F. Monti, G. Accorsi, N. Armaroli, Luminescent ionic transition-metal complexes for light-emitting electrochemical cells, Angew. Chem. Int. Ed. Engl. 51 (33) (2012) 8178–8211, https://doi.org/10.1002/anie.201201471.

[28] M.A. Rodgers, Solvent-induced deactivation of singlet oxygen: additivity relationships in nonaromatic solvents, J. Am. Chem. Soc. 105 (20) (1983) 6201–6205.

[29] T.G. St Denis, T. Dai, L. Izikson, C. Astrakas, R.R. Anderson, M.R. Hamblin, et al., All you need is light: antimicrobial photoinactivation as an evolving and emerging discovery strategy against infectious disease, Virulence 2 (6) (2011) 509–520, https://doi.org/10.4161/viru.2.6.17889.

[30] H. Ishida, S. Tobita, Y. Hasegawa, R. Katoh, K. Nozaki, Recent advances in instrumentation for absolute emission quantum yield measurements, Coord. Chem. Rev. 254 (21–22) (2010) 2449–2458.

[31] CLSI, Performance Standards for Antimicrobial Susceptibility Testing, 27 ed, ed., C.a.L.S. Institute, 2017.

[32] M. Kreitner, R. Ebermann, G. Alth, Quantitative determination of singlet oxygen. Production by porphyrins, J. Photochem. Photobiol. B: Biol. 36 (2) (1996) 109–111.

[33] D.C. Hone, P.I. Walker, R. Evans-Gowing, S. FitzGerald, A. Beeby, I. Chambrier, et al., Generation of cytotoxic singlet oxygen via phthalocyanine-stabilized gold nanoparticles: a potential delivery vehicle for photodynamic therapy, Langmuir 18 (8) (2002) 2985–2987.

[34] M.I. Gutiérrez, C.G. Martínez, D. García-Fresnadillo, A.M. Castro, G. Orellana, A.M. Braun, et al., Singlet oxygen (1Δg) production by ruthenium (II) complexes in microheterogeneous systems, J. Phys. Chem. A 107 (18) (2003) 3397–3403.

[35] D. Ashen-Garry, M. Selke, Singlet oxygen generation by cyclometalated complexes and applications, Photochem. Photobiol. 90 (2) (2014) 257–274.

[36] E. Wachter, D.K. Heidary, B.S. Howerton, S. Parkin, E.C. Glazer, Light-activated ruthenium complexes photobind DNA and are cytotoxic in the photodynamic therapy window, Chem. Commun. 48 (77) (2012) 9649–9651, https://doi.org/10.1039/C2CC33359G.

[37] F. Li, J.G. Collins, F.R. Keene, Ruthenium complexes as antimicrobial agents, Chem. Soc. Rev. 44 (8) (2015) 2529–2542, https://doi.org/10.1039/c4cs00343h.

[38] I. González, P. Dreyse, Substituent influence in phenanthroline-derived ancillary ligands on the excited state nature of novel cationic Ir(III) complexes, New J. Chem. 42 (2018) 6644–6654.

[39] T. Ganz, Defensins: antimicrobial peptides of innate immunity, Nat. Rev. Immunol. 3 (9) (2003) 710–720, https://doi.org/10.1038/nri1180.

[40] T.N. Demidova, M.R. Hamblin, Effect of cell-photosensitizer binding and cell density on microbial photoinactivation, Antimicrob. Agents Chemother. 49 (6) (2005) 2329–2335, https://doi.org/10.1128/AAC.49.6.2329-2335.2005.

[41] T. Maisch, A. Eichner, A. Spath, A. Gollmer, B. Konig, J. Regensburger, et al., Fast and effective photodynamic inactivation of multiresistant bacteria by cationic riboflavin derivatives, PLoS One 9 (12) (2014) e111792, https://doi.org/10.1371/journal.pone.0111792.

[42] G. Tortora, B. Orsini, P. Pecile, An ingestible capsule for the photodynamic therapy

of Helicobacter pylori infection, IEEE/ASME Trans. Mechatron. 21 (4) (2016) 1935–1942, https://doi.org/10.1109/TMECH.2016.2536944 IEEE/ASME.
[43] K.O. Wikene, H.V. Rukke, E. Bruzell, H.H. Tonnesen, Investigation of the antimicrobial effect of natural deep eutectic solvents (NADES) as solvents in antimicrobial photodynamic therapy, J. Photochem. Photobiol. B 171 (2017) 27–33, https://doi.org/10.1016/j.jphotobiol.2017.04.030.
[44] D. Pletzer, S.C. Mansour, R.E.W. Hancock, Synergy between conventional antibiotics and anti-biofilm peptides in a murine, sub-cutaneous abscess model caused by recalcitrant ESKAPE pathogens, PLoS Pathog. 14 (6) (2018) e1007084, https://doi.org/10.1371/journal.ppat.1007084.
[45] Y.J. Yang, S.N. Qi, R.Y. Shi, J. Yao, L.S. Wang, H.Q. Yuan, et al., Induction of apoptotic DNA fragmentation mediated by mitochondrial pathway with caspase-3-dependent BID cleavage in human gastric cancer cells by a new nitroxyl spin-labeled derivative of podophyllotoxin, Biomed. Pharmacother. 90 (2017) 131–138, https://doi.org/10.1016/j.biopha.2017.03.048.
[46] S. Anand, A. Yasinchak, T. Bullock, M. Govande, E.V. Maytin, A non-toxic approach for treatment of breast cancer and its metastases: capecitabine enhanced photodynamic therapy in a murine breast tumor model, J. Cancer Metastasis Treat. 5 (2019), https://doi.org/10.20517/2394-4722.2018.98.